ADVANCES IN FOREST FIRE RESEARCH

2022

Edited by
DOMINGOS XAVIER VIEGAS
LUÍS MÁRIO RIBEIRO

Simulation of induced-wind-dominated fire on sloping terrain

Gilbert Accary*[1]; Jacky Fayad[2]; François-Joseph Chatelon[2]; Nicolas Frangieh[2]; Carmen Awad[2]; Sofiane Meradji[3]; Thierry Marcelli[2]; Jean-Louis Rossi[2]; Dominique Morvan[4] ; Lucile Rossi[2]

[1] Scientific Research Centre in Engineering, Lebanese University. Museum Square, 1106 Beirut, Lebanon {gaccary@ul.edu.lb}
[2] UMR CNRS SPE 6134, Université de Corse – CNRS. 20250 Corte, France {fayad_j, chatelon_j.fr, frangieh_n, awad_c, marcelli_t, rossi_j, rossi_l}@univ-corse.fr
[3] IMATH laboratory, EA 2134, Toulon University. 83160 Toulon, France {sofiane.meradji@univ-tln.fr}
[4] Aix-Marseille University, CNRS, Centrale Marseille, M2P2. Marseille, France {dominique.morvan@univ-amu.fr}

**Corresponding author*

Keywords

Extreme fire; fire behavior, physical fire model; FireStar3D, numerical simulation

Abstract

Using the fully physical model FireStar3D, numerical simulations of grassland fires were carried out on a sloping terrain (10°, 25°, and 40° inclinations) for a 10 m-open wind speed of 1, 2, and 3 m/s. To reproduce the behaviour of a quasi-infinite fire front, periodic conditions were considered in the fireline direction. The simulations highlight the role played by the additional wind induced by the fire (that reaches about 10 m/s at 10 m above ground) and its feedback action on fire behaviour. This interaction results in the transition of the fire behaviour to induced-wind-dominated fire, and this goes along with a substantial increase of the fireline heat release rate that reaches 20 MW/m. In addition, the simulations highlight the acceleration of the fire spread resulting from flame attachment observed for the inclinations of 25° and 40°. The fire regime was characterized by Byram's convection number, based on the effective crosswind speed, that drops by two orders of magnitude once fire-induced wind takes effect on fire behaviour.

1. Introduction

Fire blow-up or flare-up (Viegas, 2005) is considered a very dangerous aspect of wildfire events, and is characterized by a sudden change in its behavior within a very short lapse of time. Therefore, this phenomenon presents a significant threat and one of the main causes of human losses, because of its unpredictable behavior that surprises firefighters and engulfs them with flames. There have been too many accidents imputed to blow-up fires, for instance: Mann Gulch fire in the USA, 1949 (13 victims), Storm King fire in the USA, 1994 (14 victims), Palasca in France, 2000 (2 victims), Guadalajara in Spain, 2005 (11 victims), Kornati in Craotia, 2007 (11 victims) … Many explanations have been proposed for this phenomenon (Viegas & Simeoni, 2011; Werth, 2016) and the first kind of interpretations is based on the external conditions related to stability in the atmosphere and change in the wind velocity or direction. However, real fires showed that fire blow-up could occur in the presence of contrary wind (Countryman, 1968), and laboratory experiments showed flare-up behaviors under no wind conditions (Viegas & Pita, 2004; Dold & Zinoviev, 2009). The second kind of interpretations proposed the interaction between the spreading fire and other factors like wind and topography. Indeed, the majority of blow-up fires have been observed to occur in connection with canyons or steep slopes. Thus, many models have taken into account the topographic effects in order to study flare-up behavior (Viegas, 2005; Viegas & Pita, 2004; Dold & Zinoviev, 2009; Viegas, 2006; Wu et al., 2000; Drysdale & Macmillan, 1992) and many have highlighted the role played by flame attachment to explain this fire behavior. For instance, Wu et al., 2000, carried out laboratory scale experiments on inclined surfaces and obtained a critical inclination angle of 24° for flame attachment, that separates fire spread dominated by radiative heat transfer and convective one (Dold & Zinoviev, 2009), while Drysdale & Macmillan, 1992, had noticed a change in fire behavior around 15° inclination angle. The role played by induced wind and its feed-back action on fire propagation is still an open question, but it is sure that this indraft provides oxygen to the combustion zone and contributes to fire propagation. At field scale, the accident of Freixo de Espada-a-Cinta reported by Viegas, 2005 is a good example of the presence of induced wind in a canyon. Moreover, Viegas & Pita, 2004, showed clearly the presence of

the induced wind and its effect on the fire behavior during laboratory experiments of fires spreading in canyons. In order to better understand the role played by induced wind on the behavior of fire on sloping terrain, a 3D Large Eddy Simulation (LES) was conducted using a complete physical model, namely FireStar3D (Morvan et al., 2020; Frangieh el al., 2018). The configuration was set up to allow for fire-induced wind to take place and interact consequently with the fire that induced it.

2. Modelling and Numerical Method

The mathematical model used in FireStar3D is based on a multiphase formulation (Grishin, 1997). The model consists of two parts that are solved on two distinct grids. The first part consists of the equations governing the reacting and turbulent flow of the gas mixture of fresh air and the gaseous products resulting from the degradation of the solid fuel (by drying, pyrolysis, and heterogeneous combustion) and the homogeneous combustion in the flaming zone. The second part consists of the equations governing the thermal degradation, the state and the composition, of the solid phase subjected to an intense heat flux coming from the flaming zone. The interaction between the gaseous and the solid phases, is obtained through coupling terms that appear in both parts of the model. The reader is invited to consult references (Morvan et al., 2020; Frangieh el al., 2018; Morvan & Dupuy, 2004) for more information about FireStar3D model. To avoid border effects induced by a finite-length ignition line on the fire behaviour, the simulation was carried out using periodic boundary conditions along the two lateral sides of the computational domain, as shown by Fig. 1. The homogeneous vegetation layer, of height δ = 0.6 m and whose physical properties are given in Tab. 1, is located at 30 m from the domain inlet. Domain inclination (α = 10°, 25°, or 30°) was specified through two non-zero gravity components: $g_x = -g\sin(\alpha)$ and $g_z = -g\cos(\alpha)$, where $g = 9.81$ m/s^2 is Earth gravity.

Table* 1. *Main physical properties of the vegetation

Particle density, ρ_v (kg/m^3)	1000
Volume fraction, β	0.003
Fuel moisture content, FMC (%)	60
Fuel bed depth, e (m)	0.6
Fuel load, σ (kg/m^2)	1.8
Surface-area to volume ratio, s (m^{-1})	3000
Thermal emissivity, ε	1
Fuel particles shape	Cylindrical

Initially (i.e., at t = 0), a one-seventh power horizontal velocity profile was imposed in the entire computational domain with a 10-m open wind speed U_{10} = 1, 2, or 3 m/s, and the hydrodynamic module of the code was run long enough until reaching a statistically-steady state. During this purely dynamic phase, the one-seventh power velocity profile was imposed at the domain inlet and a homogeneous Neumann outlet conditions were imposed for all primary variables of the problem. At the top boundary, a constant wind speed $U_{Top} = 1.43 \times U_{10}$ (obtained from the one-seventh power wind velocity profile) was imposed during the entire simulation time. Once the flow had reached a statistically-steady state, a 2 m wide burner was activated along the entire fuelbed width by injecting CO gas at 1600 K from the bottom boundary of the domain. The burner was activated during 10 s (at most) or until the consumption of a solid-fuel mass equal to that available above the burning area.

For the solid phase, a uniform grid with (Δx,Δy, Δz) = (0.2m, 0.2 m, 0.03 m) was used, while for the fluid phase, a uniform grid with (Δx, Δy, Δz) = (0.4 m, 0.4 m, 0.015 m) was used within the vegetation before being gradually coarsened both in the x and in the z directions. Both these grids are characterized by cells sizes below the radiation extinction length scale (Morvan, 2011) within the vegetation, given by $4/s\beta$, where s is the surface to volume ratio of the vegetation (m^{-1}) and β is the volume fraction of the solid phase (see Tab. 1); this characteristic length is equal to 0.445 m in present case. A variable time stepping strategy was used, based on a truncation-error control, with time step values varying between 0.001 s and 0.01 s. At each time step, the solution is assumed to be obtained when the residuals of all conservation equations had reached 10^{-4} in normalized form.

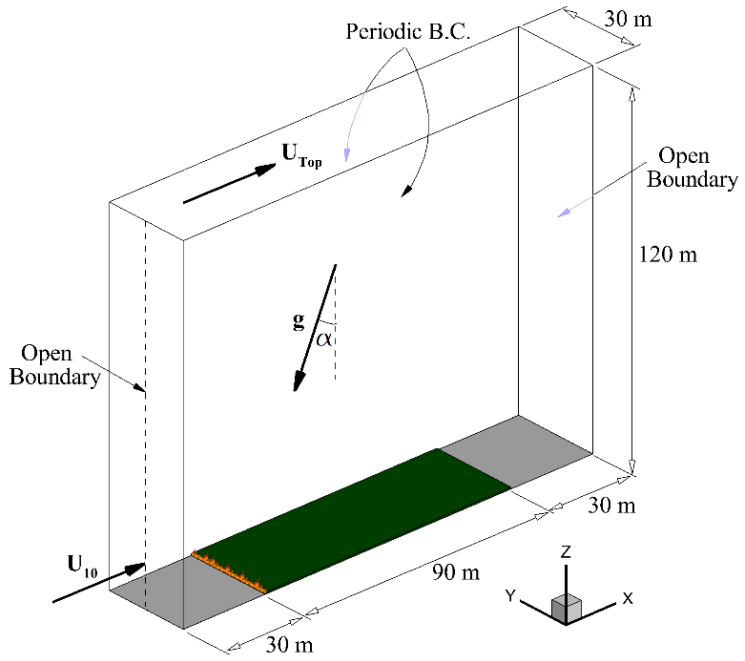

Figure 1- Computational domain and boundary conditions used to simulate an induced-wind-dominated fire on a sloping terrain.

3. Results and discussion

Figure 2 shows the time evolution of the pyrolysis front position (average at the vegetation surface), as well as the fireline heat release rate (HRR) obtained for two cases. For $\alpha = 10°$ and $U_{10} = 1$ m/s, we notice that a quasi-constant rate of spread (ROS) (the curve slope) of about 0.45 m/s is obtained, while the fireline HRR increases from about 6 to 12 MW/m after steady state of fire propagation was reached. For $\alpha = 40°$ and $U_{10} = 3$ m/s, in addition to the substantial increase of the HRR that reaches 20 MW/m, we notice a transitional phase in fire propagation where the ROS increases between 60 and 80 s after ignition from 0.5 m/s to 0.7 m/s.

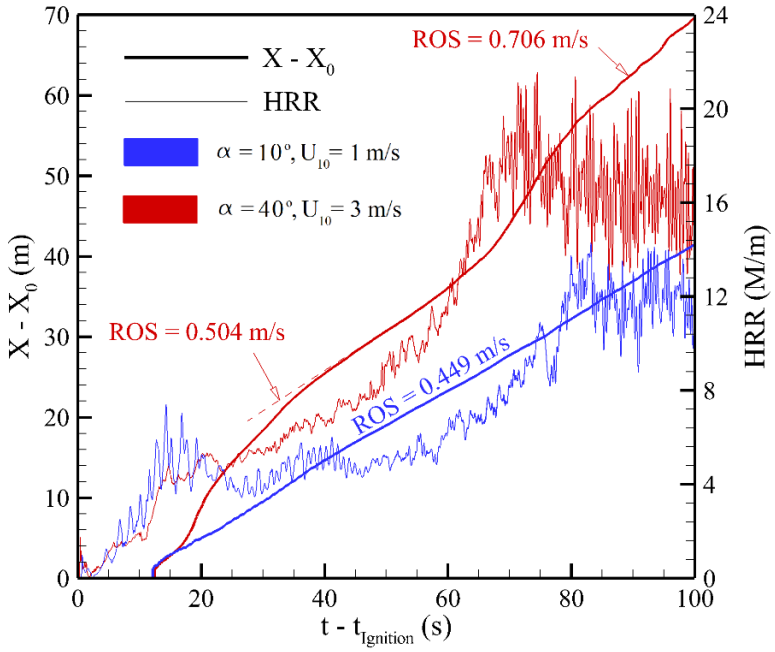

Figure 2- Time evolution of the pyrolysis front distance from burner position ($X-X_0$) and of the fireline HRR obtained for the two extreme considered cases.

To better understand the substantial increase in the HRR, figure 3(a) shows the time evolution of the 10-m open wind speed, shown in Fig. 1 at the domain inlet, for three different cases. We notice that U_{10} starts at the value imposed by the initial conditions, then it increases continuously during the simulation. This additional wind speed is induced the fire itself, it provides fresh air to the combustion zone, pushes the flames onto the unburned vegetation, and increases substantially the extend of the flaming zone, as shown in Fig. 4, and consequently the fireline HRR. Figure 3(b) shows the time evolution of the wind velocity profile along the vertical dashed-line shown in Fig. 1 at the domain inlet for $\alpha = 25°$ and $U_{10} = 2$ m/s; similar results were obtained for the other two cases. We notice how the shape of the velocity profile changes over time, with a maximum wind speed located at about 10 m above ground.

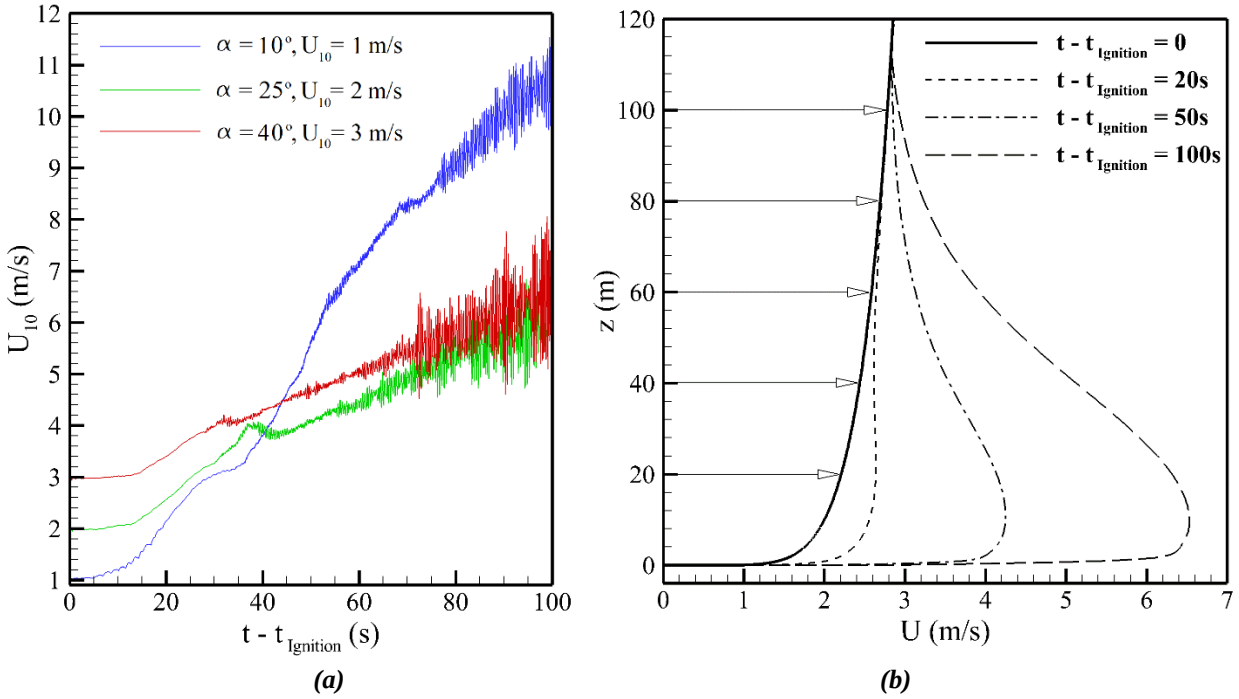

Figure 3- (a) Time evolution of the 10-m open wind speed, U_{10}, at the inlet (x = 0, y = 15 m, z = 10 m) for different simulated cases. (b) Inlet wind profile along the vertical dashed line shown in Fig. 1 at different simulation times for $\alpha = 25°$ and $U_{10} = 2$ m/s.

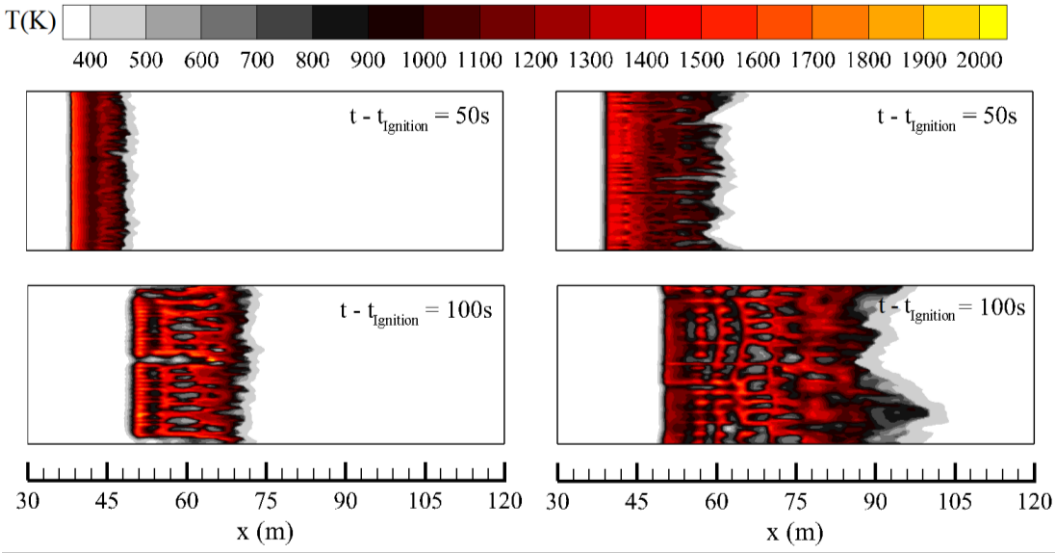

Figure 4- Distribution of the fuel particles temperature at the fuel-bed surface and for two simulation times. Left: $\alpha = 10°$ and $U_{10} = 1$ m/s, right: $\alpha = 40°$ and $U_{10} = 3$ m/s.

The transitional phase in fire propagation observed in Fig. 2 for α = 40° and U_{10} = 3 m/s (also obtained with less intensity for α = 25° and U_{10} = 2 m/s) seems to result mainly from flame attachment, as shown in Fig. 5, while it was not observed for α = 10° and U_{10} = 1 m/s, which is consistent with literature (Wu et al., 2000).

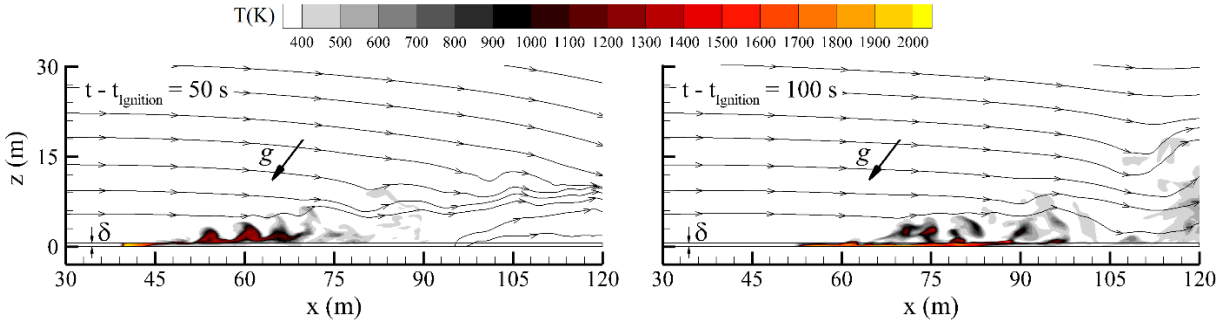

Figure 5- Temperature field and streamlines in the vertical median plane (y = 15 m) obtained for α = 40° and U_{10} = 3 m/s before ($t - t_{Ignition}$ = 50 s) and after ($t - t_{Ignition}$ = 100 s) flame attachment.

The transition between plume-dominated and wind-dominated regimes is piloted by the ratio between the two forces governing flames trajectory: buoyancy contributing to maintain the flames more or less vertical and the wind inertial force pushing the flames towards the unburned vegetation. The ratio between the power of these two forces defines a dimensionless parameter, Byram's convective number (Nelson, 2015), defined by Eq. (1).

$$N_C = \frac{2\, g\, I\, cos^3\alpha}{\rho_0\, C_{P0}\, T_0\, (U_{10}^e - ROS)^3} \tag{1}$$

where, ρ_0 and C_{P0} represent the density and the specific heat of air in standard conditions at temperature T_0, g is the acceleration of gravity, I is the fireline intensity (aberage value of the HRR), and U_{10}^e is the effective 10 m-open wind speed (accounting for the fire-induced wind). The thresholds for the transition between the two regimes of propagation are: $N_C < 2$ (wind-driven fire) and $N_C > 10$ (plume-dominated fire) (Morvan & Frangieh, 2018; Byram, 1959). Figure 6 shows the evolution time of Byram's number, obtained from Eq. (1), for the three considered cases. We notice that Byram's number decreases by the action of the additional wind induced by the fire itself and eventually corresponds to wind-driven fires for all considered cases. Also, the signature of flame attachement is visible between 60 and 80 s after ignition on the evoluation of Byram's number.

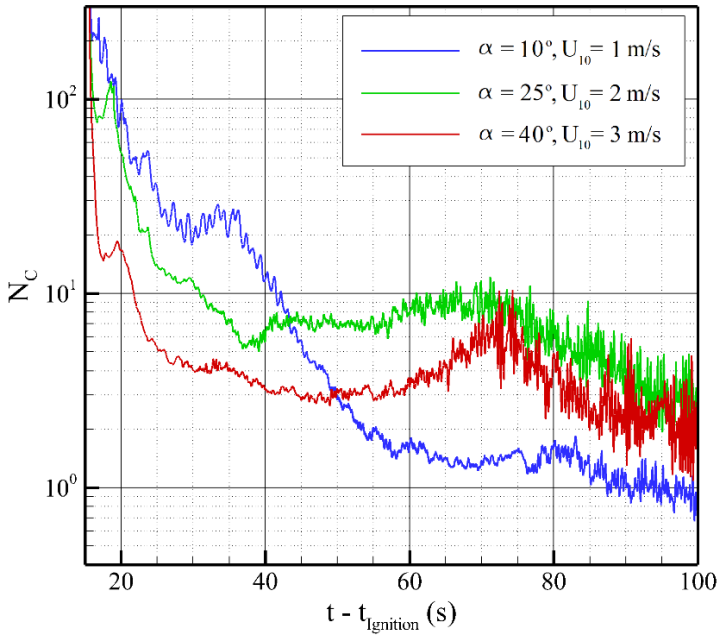

Figure 6- Time evolution of Byram's number obtained from Eq. (1) for the different simulated cases.

4. Conclusion

Induced-wind-dominated fire has been simulation numerically on a sloping terrain using FireStar3D. The action of the induced wind results within few seconds in a substantial increase of the HRR. This is coupled to the flare-up effect of flame attachment that was observed for an inclination angle higher than 25°. This study is, to our knowledge, the first to numerically demonstrate the feed-back action of fire-induced wind. This pioneering work paves the way to other numerical studies that could address open questions related to the role played by induced wind, such as: What are the conditions that favour the development of this mechanism? Does it develop in the case of a finite fireline? Answering these questions will certainly improve our understanding this type of fires and its triggering mechanisms.

5. References

Byram, G. M. (1959). Combustion of forest fuels, in: Davis, K. P. (Eds.), Forest Fire Control and Use, McGraw-Hill, New York.

Countryman, C. M., Fosberg, M. A., Rothermel, R. C., and Schroeder, M. J. (1968). Fire Weather and Fire Behaviour in the 1966 Loop Fire. Fire Technology 4, 126-41.

Dold, J. W., and Zinoviev, A. (2009). Fire Eruption through Intensity and Spread Rate Interaction Mediated by Flow Attachment. Combustion Theory and Modelling 13, 763-93.

Drysdale, D. D., Macmillan, A. J. R. (1992). Flame spread on inclined surfaces. Fire Safety Journal 18, 245-254.

Frangieh, N., Morvan, D., Accary, G., Méradji, S., Bessonov, O. (2018). Numerical simulation of grassland fires behavior using an implicit physical multiphase model. Fire Safety Journal 102, 37-47.

Grishin, A. M., Albini, F.A. (1997). Mathematical modelling of forest fires and new methods of fighting them. Publishing House of the Tomsk University: Russia.

Werth, P.A., Potter, B.E., Alexander, M.E., Clements, C.B., Cruz, M.G., Finney, M.A., Forthofer, J.M., Goodrick, S.L., Hoffman, C., Jolly, W.M., McAllister, S.S., Ottmar, R.D., Parsons, R.A. (2016). Synthesis of knowledge of extreme fire behavior: Volume 2 for Fire Behavior Specialists, Researchers, and Meteorologists, Gen. Tech. Rep. PNW-GTR-891. 258.

Morvan, D., Dupuy, J. L. (2004). Modeling the propagation of a wildfire through a Mediterranean shrub using a multiphase formulation. Combustion and Flame 138, 199-210.

Morvan, D. (2011). Physical Phenomena and Length Scales Governing the Behaviour of Wildfires: A Case for Physical Modelling, Fire Technol. 47, 437-460.

Morvan, D., Frangieh, N. Wildland fires behaviour: Wind effect versus Byram's convective number and consequences upon the regime of propagation, Int. J. Wildl. Fire. 27 (2018) 636-641.

Morvan, D., Accary, G., Méradji, S., Frangieh, N., Bessonov, O. (2020). A 3D physical model to study the behavior of vegetation fires at laboratory scale. Fire Safety Journal 101, 39-52.

Nelson, R. M. (2015). Re-analysis of wind and slope effects on flame characteristics of Mediterranean shrub fires, Int. J. Wildl. Fire. 24, 1001-1007.

Viegas, D. X., and Pita, L. P. (2004). Fire Spread in Canyons. International Journal of Wildland Fire 13, 253-274.

Viegas, D.X. (2006). Parametric study of an eruptive fire behaviour model. International Journal of Wildland Fire 15, 169-177.

Viegas, D.X. (2011). A mathematical model for forest fires blowup. Combust. Sci. Technol. 177, 27-51.

Viegas, D.X. Simeoni, A. (2011). Eruptive Behaviour of Forest Fires, Fire Technol. 47, 303-320.

Wu, Y., Xing, H. J., Atkinson, G. (2000). Interaction of fire plume with inclined surface. Fire Safety Journal 35, 391-403.